



UNIVERSITY OF LEEDS

This is a repository copy of *Non-Linear Dynamic Joint Selection Strategy for Hinge Controlled Masonry Arches*.

White Rose Research Online URL for this paper:  
<https://eprints.whiterose.ac.uk/151252/>

Version: Accepted Version

---

**Proceedings Paper:**

Stockdale, G, Sarhosis, V [orcid.org/0000-0002-8604-8659](https://orcid.org/0000-0002-8604-8659) and Milani, G (2020) Non-Linear Dynamic Joint Selection Strategy for Hinge Controlled Masonry Arches. In: AIP Conference Proceedings. 17th International Conference of Numerical Analysis and Applied Mathematics (ICNAAM 2019), 23-28 Sep 2019, Rhodes, Greece. AIP Publishing . ISBN 978-0-7354-4025-8

<https://doi.org/10.1063/5.0026431>

---

The following article has been published by AIP Conference Proceedings. It can be found at <https://doi.org/10.1063/12.0001449>. This article is protected by copyright. All rights reserved.

**Reuse**

Items deposited in White Rose Research Online are protected by copyright, with all rights reserved unless indicated otherwise. They may be downloaded and/or printed for private study, or other acts as permitted by national copyright laws. The publisher or other rights holders may allow further reproduction and re-use of the full text version. This is indicated by the licence information on the White Rose Research Online record for the item.

**Takedown**

If you consider content in White Rose Research Online to be in breach of UK law, please notify us by emailing [eprints@whiterose.ac.uk](mailto:eprints@whiterose.ac.uk) including the URL of the record and the reason for the withdrawal request.



[eprints@whiterose.ac.uk](mailto:eprints@whiterose.ac.uk)  
<https://eprints.whiterose.ac.uk/>

# Non-Linear Dynamic Joint Selection Strategy for Hinge Controlled Masonry Arches

Gabriel Stockdale<sup>1, a)</sup> Vasilis Sarhosis<sup>2, b)</sup> and Gabriele Milani<sup>1, c)</sup>

<sup>1</sup> Dept. of Architecture, Built Environment and Construction Engineering (ABC),  
Politecnico di Milano, Piazza Leonardo da Vinci 32, 20133 Milan, Italy

<sup>2</sup> School of Engineering, University of Leeds, LS2 9JT, UK

<sup>a)</sup>Corresponding author: gabriellee.stockdale@polimi.it

<sup>b)</sup>v.sarhosis@leeds.ac.uk

<sup>b)</sup>Gabriele.milani@polimi.it

**Abstract.** Masonry arches are vulnerable to seismic actions. Over the last few years, extensive research has developed strengthening strategies and methods to resist these seismic actions. However, from such studies, it is evident that the application of reinforcement to a masonry arch is done such that its failure limit is transformed from stability to a strength. This direct transformation overlooks the intermittent stages that exist, and thus provides an incomplete picture to the potential behaviors of the system. These intermittent stages can be established through subjecting the arch to hinge control and have shown the potential to increase capacity and control failure, but the computational costs for assessing the non-linear dynamic behavior of all potential mechanisms is high. This work presents a hinge-joint selection strategy from magnitude variations of short span non-linear dynamic loading through the two-dimensional Discrete Element Method (DEM) based software UDEC. Each voussoir of the arch was represented by a distinct block within the DEM. Mortar joints were modelled as zero thickness interfaces which can open and close. Twenty-five unique configurations of an arch with controlled hinges were developed and each was subjected to short duration seismic velocity profile with varying magnitudes. From this analysis an optimal hinge set with is identified.

## INTRODUCTION

Reinforcement of masonry arches is necessary for preventing seismic induced collapse. Of the various techniques, fiber reinforced polymers (FRP) and textile reinforced mortars (TRM) both focus on reinforcing the development of flexural joints. Typically, their application is designed to maximize capacity which transforms the traditional minimum mechanism analysis into a material strength problem (i.e. rupture, crushing or delamination) [1-4]. It has been revealed through considering the intermittent stages between the minimum mechanism and full strengthening under static assessments that the potential exists to increase capacity and control failure for arches subjected to hinge control [5-7]. It is now necessary to begin expanding the evaluation beyond static conditions, but non-linear dynamic loading is computationally expensive. Therefore, it is necessary to establish selection reduction strategies to reduce the number of hinge sets requiring full non-linear dynamic analyses. This work presents the numerical examination of a class of 25 admissible mechanisms for a dry-stack masonry arch subjected to hinge control and identifies the optimal hinge set configuration based upon a magnitude variation of a short-span non-linear dynamic sequence.

## ARCH MODEL

The arch model used in this investigation is a 27-block semi-circular arch whose arch and block geometry is shown in Fig. 1. Figure 2 identifies the nomenclature used for the model.

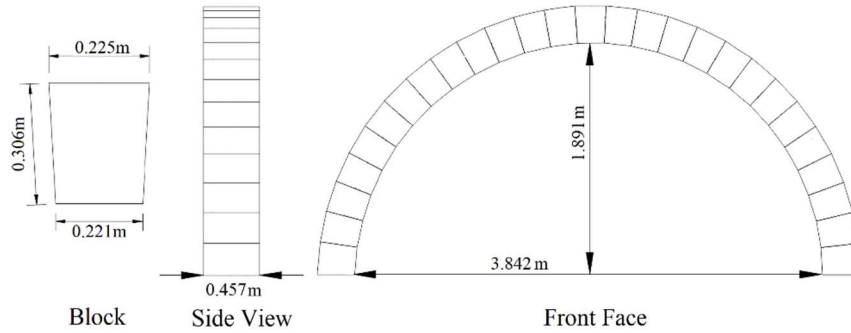


FIGURE 1. Arch model geometry and block dimensions

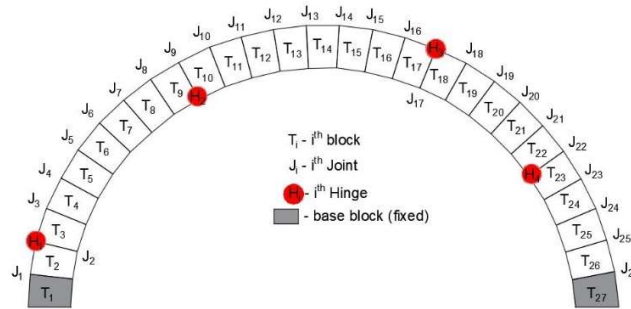


FIGURE 2. Arch model nomenclature

## DEM Overview and the Developed Model

The discrete element method (DEM) is a discontinuum analysis technique and it is presented in the UDEC (Universal Distinct Element Code) software developed by Cundall in the early 1970s for numerical research into the sliding of earth and rock masses. The software has since been used for a variety of applications. For the masonry analysis in this work, the units are represented as an assembly of rigid blocks. Rigid block geometries maintain their defined shape regardless of the loading. The mortar joints are represented as zero thickness interfaces between the blocks to model a dry-stack condition. Contact is represented by a set of points with no consideration of the stress distribution of the contact surface. Contact assignments allow the formulation of interface constitutive relations in terms of the stresses and relative displacements across the joint. The nodal displacements and block rotations are solved explicitly by differential equations from the known displacements, and Newton's second law of motion provides the motion of the blocks. Thus, large displacements and rotations of the blocks are permitted. Convergence to static solutions is obtained by means of adaptive damping, as in the classical dynamic relaxation methods.

Independent geometric models were created for the control arch model and for each tested hinge set. The control arch contained no hinge control and was modelled by 27 rigid voussoirs connected by 26 joint interfaces (see Fig. 3). Each mechanical joint set was represented by three rigid voussoirs, two rigid bases and four joints as shown in Fig. 3. All joints were defined as zero-thickness interface elements that follow the Coulomb failure criterion. A description of modelling masonry with DEM can be found at [8, 9].

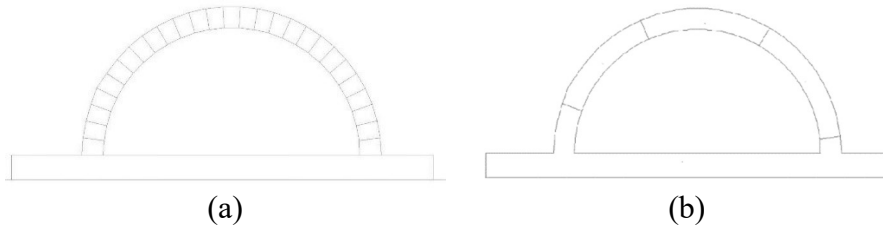


FIGURE 3. DEM model geometry for (a) the control arch and (b) a typical hinge-controlled arch

The material properties assigned to the joints of each arch model are provided in Table 1. The required material parameter for representing rigid voussoirs is the unit weight ( $d$ ), which was taken as  $550 \text{ kg/m}^3$ . Elastic-perfectly plastic coulomb slip joint area contact interfaces were used for the joints. The joint normal and shear stiffness were set high to remove potential block penetrations. To represent dry-joints, the cohesion, tensile strength and the dilatation angle of the interfaces were set to zero. Self-weight was modelled as gravitational loads.

TABLE 1. Dry-joint material properties for the DEM models

Normal Stiffness [GPa/m]	Shear Stiffness [GPa/m]	Friction Angle [°]	Cohesive Strength [kPa]	Tensile Strength [MPa]	Dilation Angle [°]
20	10	22	0	0	0

Self-weight effects were assigned as gravitational load and each model was brought into a state of equilibrium under its weight. Then, external loading was applied through the velocity component of a time history seismic sequence applied to the base of the model. Crown displacements of the arch were recorded.

## ANALYSIS PROCEDURE FOR JOINT SELECTION

The dynamic analysis procedure for identifying the optimal mechanical joint set involved a two-stage process. First, a collapse time was obtained by applying the dynamic ground velocity profile to the control arch. The collapse time established the reduced analysis duration of the dynamic loading applied to the 25 unique hinge sets established through hinge control. This was repeated at a magnitude of one, two, three, four and five times the original velocity profile. The crown and base displacements were recorded, and the final horizontal crown displacement was calculated and compared for each hinge set and earthquake scale. From the comparison, the optimal hinge configuration was identified by the hinge set with the minimum final deformation at the unreinforced collapse time.

### Earthquake Velocity Data

The ground velocity vector from Bucharest 1977 earthquake (see Fig. 4) was applied in both the horizontal and vertical directions for each analysis run. As stated, the scale of the vectors ranged from one and five times the original.

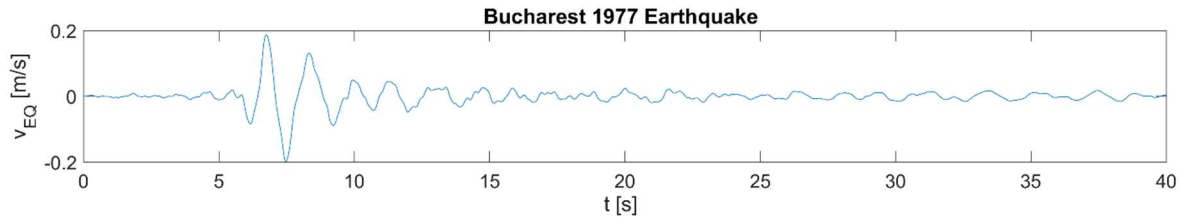


FIGURE 4. Velocity data for the 1977 Bucharest earthquake

### Hinge Sets

Tables 2 and 3 identify the 25 tested hinge sets. The selected hinge sets are the minimum configurations for the admissible locations of base hinges ( $H_1$  and  $H_4$ ) as determined through the development of a collapse load diagram [7].

TABLE 2. Hinge joint locations for hinge sets HS01 through HS10. Refer to Fig. 2 for joint identification

	HS 01	HS 02	HS 03	HS 04	HS 05	HS 06	HS 07	HS 08	HS 09	HS 10	HS 11	HS 12	HS 13
<b>H<sub>1</sub></b>	J <sub>1</sub>	J <sub>2</sub>	J <sub>3</sub>	J <sub>3</sub>	J <sub>3</sub>								
<b>H<sub>2</sub></b>	J <sub>8</sub>	J <sub>9</sub>	J <sub>9</sub>	J <sub>9</sub>	J <sub>9</sub>	J <sub>10</sub>	J <sub>10</sub>	J <sub>10</sub>					
<b>H<sub>3</sub></b>	J <sub>17</sub>	J <sub>17</sub>	J <sub>16</sub>	J <sub>16</sub>	J <sub>16</sub>	J <sub>16</sub>	J <sub>17</sub>	J <sub>17</sub>	J <sub>17</sub>	J <sub>18</sub>	J <sub>17</sub>	J <sub>17</sub>	J <sub>16</sub>
<b>H<sub>4</sub></b>	J <sub>26</sub>	J <sub>25</sub>	J <sub>24</sub>	J <sub>23</sub>	J <sub>22</sub>	J <sub>22</sub>	J <sub>23</sub>	J <sub>24</sub>	J <sub>25</sub>	J <sub>26</sub>	J <sub>26</sub>	J <sub>25</sub>	J <sub>24</sub>

**TABLE 3.** Hinge joint locations for hinge sets HS14 through HS25. Refer to Fig. 2 for joint identification

	HS 14	HS 15	HS 16	HS 17	HS 18	HS 19	HS 20	HS 21	HS 22	HS 23	HS 24	HS 25
<b>H<sub>1</sub></b>	J <sub>3</sub>	J <sub>3</sub>	J <sub>4</sub>	J <sub>3</sub>								
<b>H<sub>2</sub></b>	J <sub>9</sub>	J <sub>9</sub>	J <sub>10</sub>	J <sub>10</sub>	J <sub>10</sub>	J <sub>11</sub>	J <sub>11</sub>	J <sub>10</sub>	J <sub>10</sub>	J <sub>10</sub>	J <sub>9</sub>	J <sub>9</sub>
<b>H<sub>3</sub></b>	J <sub>16</sub>	J <sub>16</sub>	J <sub>16</sub>	J <sub>17</sub>	J <sub>17</sub>	J <sub>17</sub>	J <sub>18</sub>	J <sub>17</sub>	J <sub>17</sub>	J <sub>16</sub>	J <sub>16</sub>	J <sub>16</sub>
<b>H<sub>4</sub></b>	J <sub>23</sub>	J <sub>22</sub>	J <sub>22</sub>	J <sub>23</sub>	J <sub>24</sub>	J <sub>25</sub>	J <sub>26</sub>	J <sub>26</sub>	J <sub>25</sub>	J <sub>24</sub>	J <sub>23</sub>	J <sub>22</sub>

## RESULTS

The unreinforced collapse time was identified as the time the keystone struck the ground. This time was 5.7 seconds. Applying the collapse time to the analyses of the 25 hinge sets revealed that none of the hinge-controlled arches failed within the collapse time. This held for all magnitude increases as well. Figure 6 shows the final horizontal crown displacements of all the tests. From Fig. 6 hinge set 05 was clearly identified as the optimal hinge set.

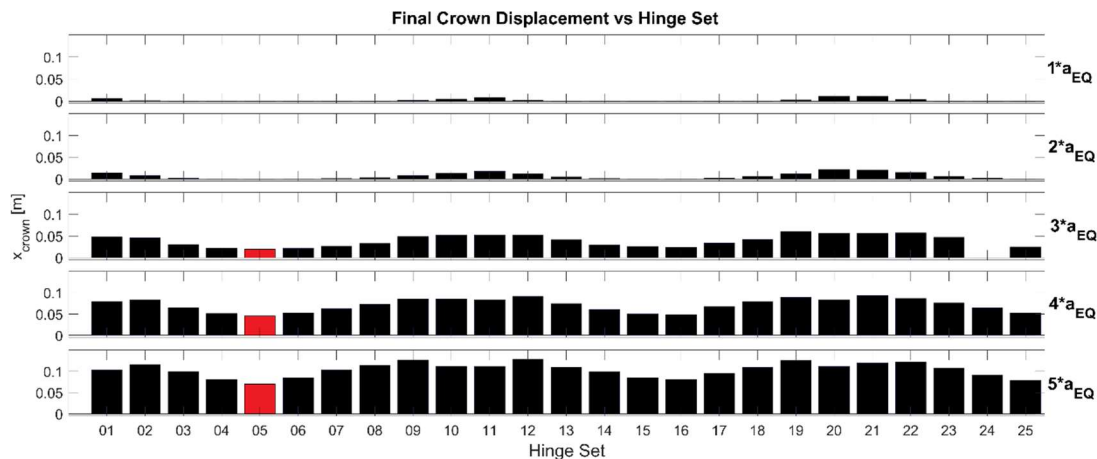


**FIGURE 5.** Final displacement versus hinge sets for all scaled dynamic analyses performed for the collapse time duration

## REFERENCES

1. E. Bertolesi, G. Milani, F.G. Carozzi and C. Poggi, Ancient masonry arches and vaults strengthened with TRM, SRG and FRP composites: Numerical analyses. *Composite Structures*, **187**, 385-402 (2018).
2. S. De Santis, F. Roscini, G. de Felice, Full-scale tests on masonry vaults strengthened with Steel Reinforced Grout. *Composites Part B*, **141**, 20-36 (2018).
3. L. Anania and G. D'Agata, Limit Analysis of vaulted structures strengthened by an innovative technology in applying CFRP. *Construction and Building Materials*, **145**, 336-346 (2017).
4. C. Modena, G. Tecchio, C. Pellegrino, F. da Porto, M. Donà, P. Zampieri and M.A. Zanini, Reinforced concrete and masonry arch bridges in seismic areas: typical deficiencies and retrofitting strategies. *Structure and Infrastructure Engineering*, **11**:4, 415-442 (2015).
5. G. Stockdale, V. Sarhosis and G. Milani, Increase in seismic resistance for a dry joint masonry arch subjected to hinge control, *10<sup>th</sup> IMC Conference Proceedings, International Masonry Society*, 968-981 (2018).
6. G. Stockdale, V. Sarhosis and G. Milani, Seismic Capacity and Multi-Mechanism Analysis for Dry-Stack Masonry Arches Subjected to Hinge Control, *Bull Earthq Eng*, (2019). <https://doi.org/10.1007/s10518-019-00583-7>
7. G. Stockdale, G. Milani and V. Sarhosis, Increase in Seismic Resistance for a Full-Scale Dry Stack Masonry Arch Subjected to Hinge Control, *Key Engineering Materials*, **817**, 221-228 (2019)
8. V. Sarhosis, K. Bagi, J.V. Lemos and G. Milani, Computational modeling of masonry structures using the discrete element method. IGI Global, USA (2016).
9. V. Sarhosis and Y. Sheng, Identification of material parameters for low bond strength masonry, *Engineering Structures*, **60**, 100-110, 2014.